Conformational study of isolated pindolol by HF, DFT and MP2 calculations

Sandra C.C. Nunes, A.J. Lopes Jesus, Mário Túlio S. Rosado, M. Ermelinda S. Eusébio *

Department of Chemistry, University of Coimbra, 3004-535, Coimbra, Portugal

Abstract

In the present work a conformational analysis of pindolol, a beta-blocker, is performed using several computational methods, including HF, DFT (B3LYP) and MP2. The relative electronic energies as well as the relevant dihedral angles of the significant conformer geometries are reported.

At the HF and DFT levels the most stable conformers of pindolol are characterized by an extended backbone structure, minimizing the steric repulsions between the indole ring and the side chain. The two backbone dihedrals, defining the position of the ring relatively to the side chain, are found to be particularly important. The lower energy structures obtained by HF and DFT also contribute significantly to the MP2 conformational population. This last method increases the stability of some conformers presenting a more folded backbone.

Most conformers exhibit hydrogen bonding. This feature, although not being the dominant factor in energetic terms, appears to be of foremost importance to define the geometry of the molecule. Four intramolecular hydrogen bonds established between the polar groups were identified by the structural geometric parameters. These involved the hydroxyl and amine functional groups and were identified and characterized by the frequency shift in their stretching vibration modes.
© 2006 Elsevier B.V. All rights reserved.

Keywords: Pindolol; Beta-blocker; Conformational analysis; Hydrogen bonding; HF; DFT; MP2

1. Introduction

The main goal of the present paper is to investigate the structure of the pindolol isolated molecule. This compound, belonging to a series of drugs commonly known as beta-blockers, is widely used in medical practice in blood pressure control and in the treatment of heart diseases [1–3].

In a previous work performed in our research group using calorimetric methods (differential scanning calorimetry and polarized light thermomicroscopy) three polymorphic forms of pindolol were identified by crystallization of the melt and two different arrangements were found to exist in the solid before being melted [4]. In either case the forms were found to have close energy, possibly due to a similar H-bond network differing among them only in the conformation of the non-polar parts. The possible existence of different conformations identified in the condensed states makes the study of the isolate molecule a worth to note issue.

Two of the most relevant sources to get a deep insight into the structure of any compound are the data supplied by X-ray for the crystalline state and the computational modeling of the gas state. In the case of pindolol the crystalline structure of a solid obtained from ethanol and methanol solutions is known [5,6]. The investigation of the isolated molecule structure, subject of the present paper, fulfills the second goal. The study of the conformational space of the isolated molecule can help to understand the possible conformations of the compound in the condensed states, besides supplying data on the gas state of the compound, which is normally the reference state for the thermodynamic properties.

* Corresponding author. Tel.: +351239854450; fax: +351239827703.
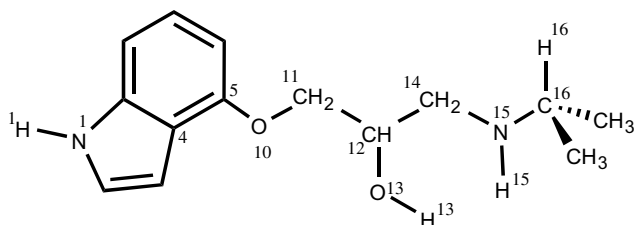 *E-mail address:* quierme@ci.uc.pt (M. Ermelinda S. Eusébio).

Fig. 1. Molecular structure of pindolol (1-(1H-Indol-4-yloxyl)-3-isopropylamino-propan-2-ol) with atom numbering scheme.

Despite the currently available computational resources, the study of molecules with the size and flexibility of those of pindolol (see Fig. 1) at a high level of theory is a hard undertaking. To reach this goal, a study of the lower energy conformers of pindolol in the gas state is performed in the present work. In order to choose the relevant conformations to investigate, among the great number of possible candidates, a conformational search method using less expensive theoretical approximations (molecular mechanics and semi-empirical calculations) is employed to generate an initial set of relevant structures of the isolated molecule. These structures are further investigated by means of HF and high-level DFT (B3LYP) and MP2 theoretical calculations, allowing the determination and comparison of the energy of the conformers, as well as the identification of the most important structural features that contribute to their stabilization. A comparison of the results obtained by the different electronic structure methods employed is also included in order to investigate the relevance of both correlation and dispersion effects in the conformers energy.

A discussion on the conformational features of the intramolecular hydrogen bonding is also given based on the geometrical parameters, as well as on the calculated infrared vibrational frequencies of the investigated conformers.

2. Computational details

The pindolol molecule has a chiral center giving rise to two enantiomers, *R* and *S*. As far as the isolated molecules are concerned both enantiomers are conformationally and energetically equivalent. In this work the calculations were only performed on the *S* enantiomer. This molecule is very flexible, having eight relevant dihedrals, six of them related to the backbone structure and two other with the OH and NH groups orientation. Assuming a three-fold rotation for each one of the dihedrals, one can obtain $3^8 = 6561$ possible minima, thus being computationally very expensive to explore all of them by means of high level electronic structure methods. Therefore, a preliminary conformational search method employing less expensive theoretical approaches was used to obtain a reasonable sampling of the most relevant conformations of pindolol.

In this work the conformational search was carried out using semiempirical (AM1) [7] and molecular mechanics (MM) methods, both employing random generation and subsequent full minimization of every internal coordinate. This random generation involved random torsion changes to the single bonds (all excluding those containing the methyl groups), followed by minimization of all internal coordinates either by molecular mechanics or semi-empirical calculations. This cycle of random changes and minimization was repeated many times until a reasonable sampling of low energy structures was obtained and for many starting structures. The molecular mechanics calculations were carried out with the CFF91 force field [8,9] using the Cerius^2 (version 3.5) molecular modeling package running on an SGI O^2/RS5000 workstation. The conformational search with the AM1 semi-empirical method was performed using the Hyperchem software [10]. Details of the conformational search methods can be found in the Cerius^2 and Hyperchem 7.5 manuals.

The generated conformations with relative energies up to 10 kJ mol^{-1} above the global minimum, corresponding to twenty structures obtained from molecular mechanics and seventeen from AM1, were then fully optimized at the Hartree-Fock (HF) level of theory using the 6-31G* basis set followed by vibrational frequencies calculation at the same level of theory. The absence of imaginary frequencies in each of the resulting conformations was used to confirm that all of them correspond to true minima on the potential energy surface.

Some folded structures initially generated by the semiempirical and MM conformational search methods converged to more extended ones after full optimization at the HF/6-31G* level. The starting structures were characterized by the possible formation of NH···π and OH···π interactions, which have been reported as relevant stabilization factors in the conformational space of other molecular systems similar to pindolol [11–14]. For this reason, it was found important to include these folded structures in the conformational analysis. However, only a few folded conformations (six) were generated by the methods used in the conformational search described above, in an energy range of *ca.* 25 kJ mol^{-1}. In order to further investigate the importance of these kind of structures in the conformational space of pindolol, a new search was performed using the PM3 semiempirical method [15,16]. All folded conformations generated by this method, within an energy range of *ca.* 25 kJ mol^{-1} (ten) were also analyzed.

A total of sixteen folded conformations (identified as E$_A$ to E$_P$) have been investigated. To maintain the NH···π and OH···π interactions throughout the HF minimization, some internal coordinates had to be frozen. Constraining some backbone torsional dihedrals was found to be inadequate, since it resulted in too high energies, not comparable with those derived by full optimization. The best alternative was to fix the distance between H$_{15}$ (NH···π) or H$_{13}$ (OH···π) and the closest aromatic carbon atom and allowing all the remaining coordinates to relax. The frozen

distance values were those obtained from semiempirical and MM minimizations (values between 2.2 and 3.1 Å, see Supplementary material).

Additional single-point calculations on the HF fully and partially optimized structures were carried out by DFT [17,18], using the B3LYP functional [19–21] and MP2 [22,23], both employing the 6-311++G** basis set. All the electronic structure calculations were performed using the Gaussian 98 program package [24].

3. Results and discussion

3.1. Structural features of the low energy conformers

Table 1 displays the conformations obtained by the methodology described above: the thirty most stable conformers fully optimized by HF and the sixteen folded conformations partially optimized (E_A to E_P). All of them are identified by six letters according to the configuration of the backbone dihedrals. The letters used are T (*trans*), G (*gauche clockwise*), G′ (*gauche anticlockwise*), corresponding to dihedrals of 180°, +60° and −60°, respectively, with a tolerance of ±60°. Two further dihedrals are required to define the orientation of O–H and N–H groups, which may play a role in the stabilization energy of the conformers by specific interactions. Fig. 2 displays some conformers of pindolol illustrating the most important features of its structure.

The values of the dihedral angles and relative electronic energies relative to the global minimum (at the HF, DFT and MP2 levels) are given in Table 1. The conformers were ordered by their DFT electronic energy. The relative energy values of the starting structures generated from the semiempirical and MM search methods are given as Supplementary material.

From the analysis of the results in Table 1, it can be noted that most of the lower energy structures predicted by HF and DFT have also a significant weight in the conformational distribution at the MP2 level. Moreover, the global minimum on the HF potential energy surface is the third lowest energy conformation (ΔE ca. 2.6 kJ mol^{-1}) at the MP2 level. Despite this, at the HF and B3LYP levels, the conformations exhibiting more extended backbones seem to be favoured, while at the MP2 level the stabilization of some of the more folded conformations occurs (see for example the geometry of E_F, E_8, E_{13} and E_{15}).

Although the molecular structure characterization of pindolol depends on the joint configuration of all dihedrals, φ_1 and φ_2, defining the position of the side chain relatively to the indole group, apparently play a crucial role in the structure of this compound. In fact, for most of the lower energy conformers, the φ_1 dihedral assumes the same *trans* configuration at all used levels of theory. This is in agreement with the theoretical and experimental results obtained for the conformational landscape of 2-phenoxy-ethanol [25], where the planar arrangement of the side chain relative to the ring (CC_{arom}–OC ≈ 0° or 180°) was found to be more stable than the perpendicular one (CC_{arom}–OC ≈ 90°).

In the case of the φ_2 dihedral, the variability is slightly more dependent on the employed method. Hence, at the HF and DFT levels the most stable conformers tend to adopt predominantly a *trans* φ_2 configuration whereas at the MP2 level some of the most stable conformers exhibit an "open" G or G′ φ_2 arrangement, with values close to 100° (see for example E_F, E_{13} and E_{15} conformations). Another relevant dihedral is φ_5, which tends to adopt preferentially a *trans* configuration at all levels of theory, corresponding to the minimum repulsive interaction between the isopropyl group and the remaining side chain. Also, the repulsive interaction between the terminal methyl and C_{14} methylene group imposes a G or G′ configuration for φ_6.

For the most stable conformers of pindolol, the remaining dihedrals take different configurations without moving φ_1, φ_2, φ_5 and φ_6 from the preferred orientations defined above.

A detailed analysis of Table 1 and Fig. 2 shows that at the HF/6-31G* and B3LYP/6-311++G** levels of theory the lower energy conformations have one or both of the middle dihedral angles in a *trans* configuration leading to a extended side chain in which the indole ring is moved away from the remaining backbone. Besides the reduction of the repulsion interactions between the side chain and the indole ring the formation of O–H···NH, O–H···O and N–H···OH intramolecular hydrogen bonds is another structural feature that should be included to explain the stability of these forms. With only a few exceptions it is worth noticing that the stability order of the conformations given by DFT closely resembles that obtained by HF. Also, the global minimum attained by the HF calculations corresponds to the lowest energy conformation after single point calculations at the DFT level.

Regarding the MP2 single point calculations, some of the folded conformations (with φ_3 and φ_4 in a G or G′ orientation), not predicted as low energy structures at the DFT and HF levels, become very stable. This is the case for E_F, E_8, E_{13}, E_{15}, E_B, E_D and E_A. The stabilization of these conformations can be, in some cases, attributed to the formation of intramolecular H-bonds between the NH group and the ether oxygen (E_8, E_{13}, E_{15}, E_B and E_A), and also to the long-range dispersion forces between the side chain and the π system of the indole ring, including possible NH···π and OH···π interactions (see Fig. 2). This effect has already shown to play an important role in the stabilization of the folded conformers of various molecules with a structure similar to that of pindolol [11,12,14,26].

The differences between DFT and MP2 in predicting the most significant conformations of molecular systems similar to pindolol have been reported by some authors [14,26]. It is generally accepted that the commonly used density functionals, such as B3LYP, tend to underestimate dispersion effects which may play a role in the conformational stability of aromatic organic molecules.

Table 1
Electronic energies (ΔE, kJ mol^{-1}) at the HF/6-31G*, B3LYP/6-311++G** and MP2/6-311++G** levels relative to the global minimum and dihedral angles of the most significant conformations of pindolol. The B3LYP and MP2 energies were obtained from single-point calculations on the HF optimized structures [a]

Conf.[b]	Label	ΔE (kJ mol^{-1})			φ_1	φ_2	φ_3	φ_4	φ_5	φ_6	φ_7	φ_8
		HF	B3LYP	MP2								
E_1	TTTG′ TG	0.00	0.00	2.59	179	−177	−180	−60	−174	47	−48	−52
E_2	TTTTTG′	3.27	1.13	6.63	180	−177	179	177	172	−48	−55	49
E_3	TTG′ TTG′	0.35	1.31	5.55	180	−180	−64	−175	162	−56	162	−73
E_4	TTG′ TTG	1.77	1.84	5.25	180	−180	−65	−176	169	42	162	−69
E_5	TTG′G′TG	2.14	2.43	3.35	180	−179	−58	−66	−156	56	86	80
E_6	TTTG′ TG′	1.29	2.52	6.63	179	−177	−179	−58	176	−53	−48	−58
E_7	TTG′G′ TG′	3.79	3.05	3.10	180	−179	−57	−65	−159	−40	86	78
E_8	TTGG′ TG	4.75	3.29	0.27	−173	176	60	−78	−162	55	90	71
E_9	TTTG TG′	5.49	5.74	9.63	180	−178	178	63	−177	−44	−49	61
E_{10}	TTG TTG′	8.12	5.92	9.41	−178	178	53	−178	162	−55	163	−73
E_{11}	TTTG TG	4.93	6.11	11.63	180	−178	178	64	−167	56	−49	68
E_{12}	TG′G′ TTG′	6.89	6.43	7.78	−177	−86	−63	−175	163	−56	162	−72
E_{13}	TGGG′ TG	8.56	7.89	3.49	146	111	54	−80	−162	55	96	70
E_{14}	TTGGTG	7.60	8.29	10.61	−180	178	68	66	−162	56	47	73
E_{15}	TGGG′ TG′	9.93	8.54	3.74	145	111	54	−79	−168	−42	96	68
E_{16}	TTG′ G′ TG	11.70	11.28	12.68	180	179	−69	−63	−179	46	−67	−56
E_{17}	GTG′ TTG′	8.18	13.89	14.00	91	−178	−64	−175	162	−56	162	−73
E_{18}	G′ TTG′ TG′	8.14	14.05	20.37	−98	−177	179	−59	176	−53	−49	−58
E_{19}	TTTTG′ G′	16.78	14.07	13.66	180	−177	179	−176	−95	−55	−54	37
E_{20}	GTG′ G′ TG	10.41	15.95	12.69	90	−174	−57	−67	−156	56	86	79
E_{21}	TGTG′ TT	16.45	16.24	16.68	177	88	177	−59	179	175	−47	−56
E_{22}	TTGTG′G′	18.53	17.23	21.40	−180	177	65	−178	−99	−56	51	31
E_{23}	TTG′GTG′	17.00	17.89	18.93	176	−179	−64	79	172	−54	−170	−61
E_{24}	TTG′GTG′	19.27	19.77	21.29	177	−179	−67	76	171	−53	−74	−62
E_{25}	G′TGTG′G	16.94	21.06	18.32	−81	165	67	−180	−78	41	52	47
E_{26}	TTG′TG′ G′	23.78	22.07	26.68	−180	−179	−63	−179	−103	−56	71	26
E_{27}	TTGG′G′G	25.74	23.17	20.34	−167	173	74	−68	−90	46	50	40
E_{28}	G′TGTG′G′	22.78	27.70	25.61	−81	164	67	−177	−99	−56	54	31
E_{29}	GTGTG′G′	24.19	28.16	27.11	95	177	66	−177	−99	−56	51	32
E_{30}	GTGTG′TG′	25.42	30.19	24.21	85	178	86	−55	−172	−50	29	−47
E_A	TGGG′TG′	14.42	13.88	4.24	171	93	56	−75	−164	−41	80	71
E_B	TGGG′TG	13.69	14.01	3.82	175	90	55	−76	−159	55	80	74
E_C	TG′TG′TG′	13.71	16.39	15.98	−158	−109	179	−61	174	−54	−50	−60
E_D	GTG′G′TG	16.62	20.13	7.24	59	130	−56	−61	−157	56	83	78
E_E	TGGGTG′	21.09	21.84	19.51	170	98	56	55	155	−56	56	−81
E_F	TG′GG′TG	28.52	22.23	0.00	173	−99	61	−75	−161	55	89	73
E_G	TG′G′GTG′	27.65	26.00	23.24	−175	−86	−59	74	169	−53	72	−63
E_H	G′G′TG′TT	26.61	28.33	21.42	−67	−89	−166	−58	179	175	−53	−56
E_I	TGGTG′G	29.76	28.95	20.75	−122	100	63	−180	−79	40	53	45
E_J	G′G′GGTG	36.84	32.04	11.40	−48	−82	73	56	158	41	44	−79
E_K	TG′G′GTT	39.20	36.93	27.28	162	−77	−56	76	168	173	72	−64
E_L	TTGG′TG′	38.91	37.24	16.47	144	−132	83	−35	−178	−46	36	−49
E_M	TTGG′G′G	39.40	38.83	29.25	−132	−139	71	−65	−94	40	52	35
E_N	TG′GG′G′G	41.96	38.84	28.09	−154	−95	72	−66	−89	40	52	42
E_O	GGGTG′T	43.52	42.02	34.78	66	88	56	−179	−99	173	53	31
E_P	G′TGG′G′G′	57.95	53.06	37.50	−38	−130	81	−54	−117	−46	47	19

[a] $\varphi_1 = C_4C_5O_{10}C_{11}$, $\varphi_2 = C_5O_{10}C_{11}C_{12}$, $\varphi_3 = O_{10}C_{11}C_{12}C_{14}$, $\varphi_4 = C_{11}C_{12}C_{14}N_{15}$, $\varphi_5 = C_{12}C_{14}N_{15}C_{16}$, $\varphi_6 = C_{14}N_{15}C_{16}H_{16}$, $\varphi_7 = C_{11}C_{12}O_{13}H_{13}$, $\varphi_8 = C_{12}C_{14}N_{15}H_{15}$.
[b] Conformations E_1 to E_{30} were fully optimized at HF/6-31G* level while conformations E_A to E_P were partially optimized at the same level.

The two most stable conformations at the MP2 level, E_F and E_8, are presented in Fig. 2. The conformational arrangement of E_8 (like E_{13} and E_{15}) enables the formation of an intramolecular H-bond between the NH group and the ether oxygen (NH···O) as well as the OH···N bond. In the case of E_F an additional interaction between the NH group and the π system is also possible. The main difference between the two conformations (see dihedral labels in Table 1), lies in the orientation of ϕ_2 (176° in E_8 and −99° in E_F), which increases the folding of E_F relatively to E_8. It is worth noticing that E_F converges to E_8 after full HF optimization.

Unlike the conformations mentioned above, some other folded ones, displayed in Table 1, present high relative energy values, even at the MP2 level (E_O, E_N, E_I, E_H, E_P, E_K, and E_M). In such cases, the stabilization due to disper-
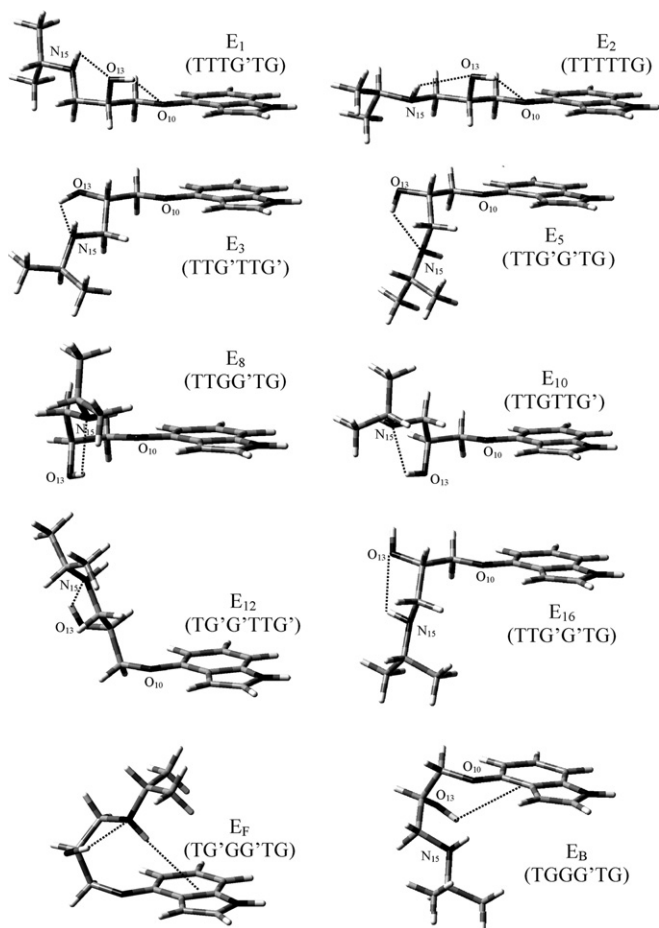
Fig. 2. Optimized geometries (HF/6-31G*) of some conformations of pindolol in the gas phase illustrating different types of backbone arrangements and intramolecular H-bonds. E_1 to E_{16} correspond to fully optimized structures; E_B and E_F were partially optimized.

Fig. 3. Potential energy profile as a function of φ_1 and φ_2 (with φ_1 fixed at 180°) using a 30° scanning step. E_1 was used as starting structure in both scans. At each point all the remaining internal coordinates were relaxed at the HF/6-31G* level of theory followed by B3LYP/6-311++G** single-point calculation.

sion interactions is overcome by unfavourable configurations resulting from the deviation of φ_1, φ_2, φ_5 and φ_6 from their preferred orientations.

The particular role played by the φ_1 and φ_2 torsional angles in the characterization of the backbone structure of pindolol deserves a detailed study, namely by mapping the potential energy profile around these two coordinates. As these two dihedrals do not seem to be particularly dependent on the calculation method used and since HF and DFT are computationally less expensive than MP2, this study was undertaken using the former methods. Taking E_1 as the starting structure, successive rotations about φ_1 using a 30° scanning step were performed. At each point all the remaining structural parameters were optimized at the HF/6-31G* level of theory followed by a B3LYP/6-311++G** energy calculation. The resulting potential energy profile is depicted in Fig. 3. The minimum energy occurs at $\varphi_1 \approx 180°$. Two other minima at $\varphi_1 = 90°$ and $\varphi_1 = -90°$ with energies of *ca.* 12 kJ mol^{-1} above the first were also observed. As φ_1 approaches 0° the energy increases due to the repulsive interaction between the side chain of the molecule and the pyrrol aromatic ring moiety.
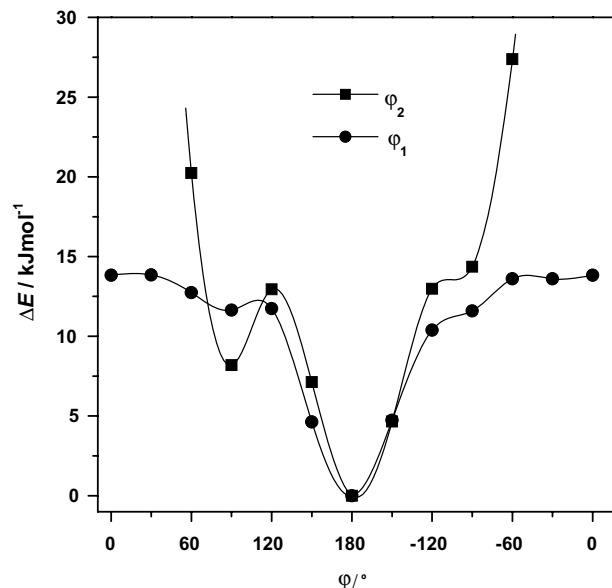
Following an identical methodology the potential energy profile around φ_2 with φ_1 fixed at 180° was obtained and is represented in Fig. 3. The potential energy pattern is akin to that around φ_1 with the lowest minimum energy occurring at $\varphi_2 = 180°$ and two higher energy minima at $\varphi_2 = 90°$ and $-90°$ of *ca.* 8 and 14 kJ mol^{-1}, respectively, above the lowest energy minimum. For $\varphi_2 < 90°$ or $\varphi_2 < -90°$ the side chain rotation is hindered by the benzenoid ring moiety.

As it was already mentioned above, we are not aware of any experimental or theoretical study performed on pindolol in the gas phase to be compared with our results. The only structural data about this compound available in literature are referred to its crystalline structure [5,6]. It is interesting to note that the conformation of pindolol exhibited in the crystal is very close to E_2, the second most stable conformer predicted by our DFT theoretical calculations.

3.2. Geometric parameters related to intramolecular hydrogen bonding

As it has been mentioned before, a structural feature accounting to the definition of the minima on the potential energy surface of pindolol is the establishment of hydrogen bonds between the polar groups. The hydroxyl and amine groups are able to act both as hydrogen donors (D) or acceptors (A) whereas the ether oxygen is only acceptor. In what follows, a detailed discussion concerning H-bonding for the sixteen lowest energy conformers at the DFT and MP2 levels is undertaken, as they account for all the different types of H-bonds in the HF fully optimized struc-

tures. The NH$\cdots\pi$ and OH$\cdots\pi$ interactions cannot be included in this discussion since they are not present in the fully optimized structures and mostly because the H$\cdots\pi$ distance, the most important parameter to be used in the discussion of this type of interactions, either from the viewpoint of geometrical considerations or from the analysis of the vibrational frequencies, corresponds to a non-optimized parameter at the HF level of theory.

On structural grounds, H-bonding is evidenced by short H$\cdots$A distances and favourable D–H$\cdots$A angles. Distances up to 3.0-3.2 Å should be accepted as a manifestation of an H-bond [27]. The directional and soft characteristics of the H-bond interaction lead to values close to linearity for the preferred orientation, but still present for D–H$\cdots$A angles >110° or even smaller [28]. We must recognize that cut-off values of the H-bond are conventional, since no definite separation exists between the H-bond and the van der Waals interactions [29,30]. As H-bonding depends on the H$\cdots$A distance and D–H$\cdots$A angle, a plot of these parameters can give an elucidative view of this type of interaction in pindolol. This representation is found in Fig. 4.

All conformers exhibit geometrical parameters acceptable for the formation of intramolecular H-bonds. In Table 2 are presented the conformers with only one H-bond and the combination of dihedral orientations leading to favourable positions of the donor and acceptor groups. While some pindolol conformers present only one of the H-bond types described in Table 2, some of the others exhibit simultaneously two of these (*e.g.*, E_1, E_2 and E_6) and in a few cases the occurrence of O_{13}–$H_{13}\cdots N_{15}$ results from a structure favouring the N_{15}–$H_{15}\cdots O_{10}$ interaction (*e.g.*, E_8, E_{13} and E_{15}).

Several bond sets are evidenced in Fig. 4. Eight conformers with D–H$\cdots$A angles ranging from 108 to 101° and H$\cdots$A distances varying between 2.25 and 2.48 Å exhibit individually or simultaneously O_{13}–$H_{13}\cdots O_{10}$ or N_{15}–$H_{15}\cdots O_{13}$ bonds. As the geometric parameters are very close to the cutoff limits, these should be classified

Table 2
Intramolecular hydrogen bonds exhibited in pindolol and dihedral angle orientations leading to their formation

H-bond	Dihedral orientations	Conformers[a]
$O_{13}H_{13}\cdots O_{10}$	(φ_3 T and φ_7 G′) or (φ_3 G and φ_7 G)	E_9, E_{11}, E_{14}
$O_{13}H_{13}\cdots N_{15}$	(φ_4 T and φ_7 T) or (φ_4 G′and φ_7 G)	E_3, E_4, E_5, E_7, E_{10}, E_{12}
$N_{15}H_{15}\cdots O_{13}$	φ_4 G′, φ_7 G′, φ_8 G′	E_{16}

[a] Conformers presenting only the considered H-bond.

as weak H-bonds. Between these two bonds, O_{13}–$H_{13}\cdots O_{10}$ is favoured over N_{15}–$H_{15}\cdots O_{13}$ and a variability of strength is expected for each of them, as can be confirmed by the diversity of angles and distances.

The O_{13}–$H_{13}\cdots N_{15}$ bond is found together with N_{15}–$H_{15}\cdots O_{10}$ (E_8, E_{13} and E_{15}) or alone (E_3, E_4, E_5, E_7, E_{10} and E_{12}) in a range of H-bond angles from 118 to 113° and in distances from 2.16 to 2.32 Å. An almost linear decrease of the angles with the increase of distance is observed. The H-bond parameters are more favourable when both bonds coexist than when the first is the only one present, as would be expected from the H-bond cooperativity effect [27,31,32]. Although differences between the conformers are expected owing to their structural features, this H-bond is stronger than those considered in the previous group of conformers.

Finally, the N_{15}–$H_{15}\cdots O_{10}$ that accompanies the O_{13}–$H_{13}\cdots N_{15}$ in the conformers E_8, E_{13} and E_{15} gives rise to stronger H-bonds in pindolol attending to the favoured donor–acceptor orientation and relatively short distances, these conformations being particularly stabilized at the MP2 level.

Two important conclusions are taken from the data given above on H-bonding in pindolol: all the conformers present, at least, one H-bond in a relative wide strength range and no correlation can be established between the H-bonding parameters and the electronic energy of the conformers. This means that this interaction is not the dominant factor in the energy ordering of the different conformers of pindolol.

3.3. H-bonding manifestation from calculated vibrational spectra

Infrared spectroscopy is a privileged method to supply details on H-bonding. This particularity is explored now to complement the data obtained on the structure parameter grounds. For these purposes, the vibrational frequencies of the fully HF optimized conformers were calculated.

One of the spectroscopic features relating H-bond with vibration modes is the stretching frequency shift defined by

$$\Delta\bar{v} = \bar{v}_{\text{D–H}\cdots\text{A}} - \bar{v}_{\text{D–H}}$$

where $\bar{v}_{\text{D–H}}$ and $\bar{v}_{\text{D–H}\cdots\text{A}}$ are the wavenumber band maximum for the free group and for the group involved in the
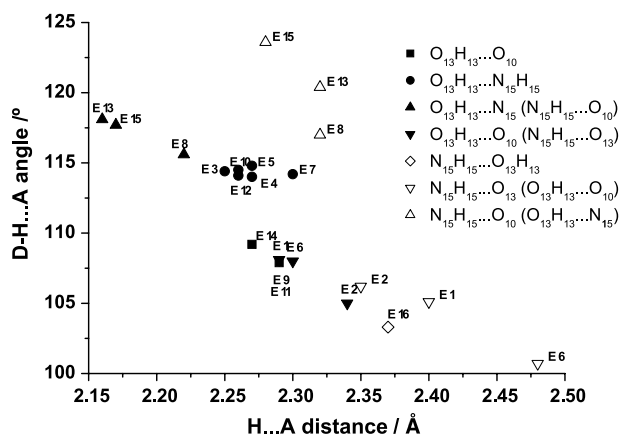

Fig. 4. Hydrogen bond angle vs. distance for conformers E_1 to E_{16}. The H-bonds accompanying that one under consideration are indicated in parentheses.
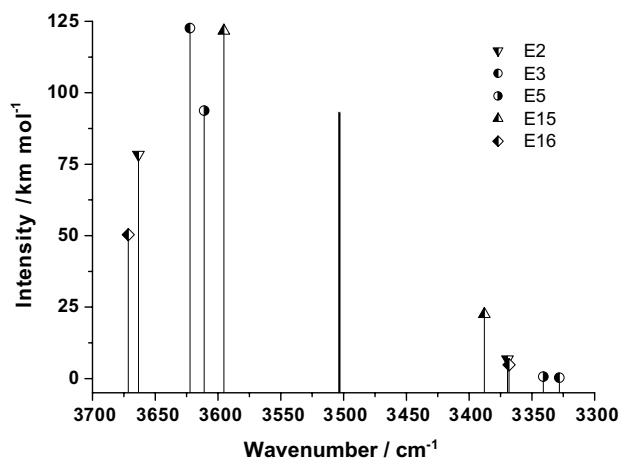
Fig. 5. Calculated spectra (HF/6-31G*) of some conformers of pindolol in the OH and NH stretching regions. The line at *ca.* 3500 cm^{-1} is assigned to the indole NH group. The lines to the right correspond to the amine NH and the ones to the left to OH.

H-bond, respectively. The $\bar{\nu}$ shift is normally more pronounced for the stretching vibration modes.

Fig. 5 presents typical spectra of some pindolol conformers in the 3700 –3200 cm^{-1} region. The wavenumbers were scaled by a factor of 0.8929 [33]. In this frequency range, the O_{13}–H_{13}, N_1–H_1 and N_{15}–H_{15} stretching vibration modes are observed. While $\bar{\nu}$ (N_1–H_1) appears at *ca.* 3500 cm^{-1} for all conformers, variation from one conformer to another occurs for the two other groups. The stretching vibration of the NH secondary amine is vanishingly weak. However, when this group acts as a donor in an H-bond formation, in addition to the stretching frequency displacement, the intensity increases.

The stretching vibration frequencies of the $O_{13}H_{13}$ and $N_{15}H_{15}$ free groups are calculated as 3671 and 3328 cm^{-1}, obtained from E_{16} and E_3, respectively. In Table 3, the values of $\Delta\bar{\nu}$ found for $O_{13}H_{13}$ and $N_{15}H_{15}$

Table 3
Stretching vibration wavenumber shifts of $O_{13}H_{13}$ and $N_{15}H_{15}$

Conformer	$\Delta\bar{\nu}$ / cm^{-1}	
	O_{13}–H_{13}	N_{15}–H_{15}
E_1	−15.8	34.4
E_2	−10.5	39.8
E_3	−51.5	–
E_4	−47.0	10.2
E_5	−62.8	11.3
E_6	−15.6	25.9
E_7	−58.9	27.5
E_8	−59.5	50.4
E_9	−13.2	11.8
E_{10}	−49.3	–
E_{11}	−12.7	–
E_{12}	−52.2	–
E_{13}	−85.4	44.7
E_{14}	−21.5	–
E_{15}	−78.5	58.3
E_{16}	–	38.7

in the sixteen conformers of pindolol, are reported. This table shows that most of the sixteen conformers present displacements of the stretching vibration of O_{13}–H_{13} and N_{15}–H_{15}. However, while the former group originates red shifts, the latter gives rise to blue shifts. From a simplistic model, a red shift would be the expected effect as far as the D–H$\cdots$A interaction increases the D–H bond length. Blue shift has been described in C–H$\cdots$O, C–H$\cdots\pi$ and N–H$\cdots$O systems [34–36]. The explanations advanced for the blue shift effect were reviewed by Alabugin et al. [37]. These authors outlined a model in which the H-bonding stabilization results from the transfer of electron lone pairs of the acceptor to an antibonding D–H orbital (hyperconjugative $n(A) \rightarrow \sigma^*(D–H)$ interaction) and also from the increase of s-character and polarization of D–H bond. The former decreases the bond order while the latter produces the opposite effect. The direction of the wavenumber shift depends on the balancing of both effects.

Although $\Delta\bar{\nu}$ is bond strength dependent and some expressions have been worked out to relate $\Delta\bar{\nu}$ with the interaction enthalpy for intermolecular H-bonding [38], it is not safe to use these expressions for red and blue shifts in intramolecular H-bonds. The strength of the H-bonds is therefore expressed in $\Delta\bar{\nu}$ values.

The values tabled for $\Delta\bar{\nu}$ show that most of the pindolol conformers exhibit H-bonds. The O_{13}–$H_{13}\cdots N_{15}$ and N_{15}–$H_{15}\cdots O_{10}$ are the main specific interactions of the H-bonding network of pindolol. These two H-bonds coexist in some conformers. The $\Delta\bar{\nu}$ values observed for N_{15}–$H_{15}\cdots O_{13}$ are not far below those found for N_{15}–$H_{15}\cdots O_{10}$ and that interaction is present in several conformers together with O_{13}–$H_{13}\cdots O_{10}$ (E_1, E_2, E_6) or alone as in E_{16}. On the grounds of the $\Delta\bar{\nu}$ values, the last H-bond is a very weak one.

The general view on H-bonding supplied by Table 3 is in accordance with the D–H$\cdots$A angles and H$\cdots$A distances displayed in Fig. 4. However, it should be pointed out that the spectroscopic manifestations of the H-bonds give more quantitative and clear indications on these interactions than the geometric parameters. Bearing this in mind, it is worth to note the different dependence on these parameters observed for the most important H-bond systems of pindolol. Plotting $\Delta\bar{\nu}$ against D–H$\cdots$A angle or H$\cdots$A distance (data provided as Supplementary material) allows to conclude that while O_{13}–$H_{13}\cdots N_{15}$ is strongly dependent on donor–acceptor orientation, the N_{15}–$H_{15}\cdots O_{10}$ is less dependent on the orientation but strongly dependent on H$\cdots$A distance. This different behaviour derives from the different nature of the bonds as referred above.

4. Concluding remarks

The structure of the isolated pindolol molecule was determined at the HF/6-31G* level of theory and the corresponding energy calculated at the B3LYP/6-311++G(d,p) and MP2/6-311++G(d,p) levels. The structures of the most significant conformers were reported as well as their

respective values of the electronic energy at the different electronic structure methods employed.

According to the energy ordering of the conformers, it can be concluded from our results that while DFT method favours more extended structures, MP2 stabilizes some of the more folded ones. However, most of the lower energy conformations predicted by HF and DFT have also a significant weight in the conformational distribution at the MP2 level. From the combination of the results obtained from the different methods, the most significant structural features of pindolol were identified and discussed.

Intramolecular H-bonds, although not the energetically dominant structural feature, play a key role in the structural stabilization of most of pindolol conformers that were studied, either on the grounds of geometric parameters or from the stretching vibration shifts of O–H and N–H bonds.

Acknowledgements

Appendix A. Supplementary data

Supplementary data associated with this article can be found, in the online version, at doi:10.1016/j.theochem.2006.11.029.

References

[1] G. Bachour, H. Losse, F. Bender, F. Wessels, Med. Klin. 71 (1976) 580.
[2] J. Holmboe, P. Lilleåsen, E. Normann, Acta Anaesthesiol. Scand. 20 (1976) 70.
[3] J.H. Atterhog, H. Duner, B. Pernow, Am. J. Med. 60 (1976) 872.
[4] S.C.C. Nunes, M.E.S. Eusébio, M.L.P. Leitão, J.S. Redinha, Int. J. Pharm. 285 (2004) 13.
[5] M. Gadret, M. Goursolle, J.M. Leger, J.C. Colleter, Acta Crystallogr. Sect. B 32 (1976) 17.
[6] T.K. Chattopadhyay, R.A. Palmer, D. Mahadevan, J. Chem. Crystallogr. 25 (1995) 195.
[7] M.J.S. Dewar, E.G. Zoebisch, E.F. Healy, J.J.P. Stewart, J. Am. Chem. Soc. 107 (1985) 3902.
[8] M.J. Hwang, T.P. Stockfisch, A.T. Hagler, J. Am. Chem. Soc. 116 (1994) 2515.
[9] J.R. Maple, U. Dinur, A.T. Hagler, Proc. Natl. Acad. Sci. USA 85 (1988) 5350.
[10] Hyperchem 7.5 for windows (Evaluation version), Hypercube Inc.
[11] J.M. Bakker, C. Plutzer, I. Hunig, T. Haber, I. Compagnon, G. von Helden, G. Meijer, K. Kleinermanns, Chem. Phys. Chem. 6 (2005) 120.
[12] I. Hunig, K. Kleinermanns, Phys. Chem. Chem. Phys. 6 (2004) 2650.
[13] D. Toroz, T. Van Mourik, Mol. Phys. 104 (2006) 559.
[14] H. Valdes, D. Reha, P. Hobza, J. Phys. Chem. B 110 (2006) 6385.
[15] J.P. James, J. Stewart, Comput. Chem. 10 (1989) 209.
[16] J.P. James, J. Stewart, Comput. Chem. 10 (1989) 221.
[17] P. Hohenberg, W. Kohn, Phys. Rev. B 136 (1964) B864.
[18] W. Kohn, L.J. Sham, Phys. Rev. 140 (1965) 1133.
[19] A.D. Becke, Phys. Rev. A 38 (1988) 3098.
[20] A.D. Becke, J. Chem. Phys. 98 (1993) 5648.
[21] C.T. Lee, W.T. Yang, R.G. Parr, Phys. Rev. B 37 (1988) 785.
[22] M.J. Frisch, M. Head-Gordon, J.A. Pople, Chem. Phys. Lett. 166 (1990) 275.
[23] M.J. Frisch, M. Head-Gordon, J.A. Pople, Chem. Phys. Lett. 166 (1990) 281.
[24] M.J. Frisch, et al., Gaussian 98, revision A.9, Gaussian, Inc, Pittsburgh, PA, 1998.
[25] N.A. Macleod, J.P. Simons, Chem. Phys. 283 (2002) 221.
[26] T. van Mourik, P.G. Karamertzanis, S.L. Price, J. Phys. Chem. A 110 (2006) 8.
[27] G.A. Jeffrey, An Introduction to Hydrogen Bonding, Oxford University Press, Oxford, 1997.
[28] T. Steiner, Angew. Chem.-Int. Edit. 41 (2002) 48.
[29] T. Steiner, G.R. Desiraju, Chem. Commun. (1998) 891.
[30] N.N.L. Madhavi, G.R. Desiraju, A.K. Katz, H.L. Carrell, A. Nangia, Chem. Commun. (1997) 1953.
[31] M.L. Paz, G. Ellis, M. Pérez, J. Perkins, J. Jiménez-Barbero, C. Vicent, Eur. J. Org. Chem. 2002 (2002) 840.
[32] J.L. Dashnau, K.A. Sharp, J.M. Vanderkooi, J. Phys. Chem. B 109 (2005) 24152.
[33] A.P. Scott, L. Radom, J. Phys. Chem. 100 (1996) 16502.
[34] H. Matsuura, H. Yoshida, M. Hieda, S.-y. Yamanaka, T. Harada, K. Shin-ya, K. Ohno, J. Am. Chem. Soc. 125 (2003) 13910.
[35] P. Hobza, Z. Havlas, Chem. Phys. Lett. 303 (1999) 447.
[36] H.M. Muchall, J. Phys. Chem. A 105 (2001) 632.
[37] I.V. Alabugin, M. Manoharan, S. Peabody, F. Weinhold, J. Am. Chem. Soc. 125 (2003) 5973.
[38] A.V. Iogansen, Spectrochim. Acta, Part A 55 (1999) 1585.